ELSEVIER

Pattern Recognition Letters 18 (1997) 269–281

Pattern Recognition Letters

Image registration by control points pairing using the invariant properties of line segments [1]

Wen-Hao Wang, Yung-Chang Chen *

Institute of Electrical Engineering, National Tsing Hua University, Hsinchu, Taiwan 30043, ROC

Received 23 April 1996; revised 9 December 1996

Abstract

A novel control points pairing algorithm for image registration is proposed in this paper. The method exploits the invariant relations between line segments of a reference and an observed image, respectively. Each segment incorporates two control points, i.e., the centroids of closed-boundary regions. By means of the invariant properties, the control points can be correctly paired. It is shown that the proposed method is simple and efficient in practical implementation. © 1997 Elsevier Science B.V.

Keywords: Image registration; Control points; Invariant properties; Line segments

1. Introduction

Image registration is the most important task for matching images of the same scene acquired at different times, from different sensors, or from different viewpoints. In the survey (Brown, 1992, p. 328), registration techniques include three principal areas:

1. **Remotely Sensed Data Processing** – target location and identification, military applications, geology, and oil exploration.
2. **Computer Vision and Pattern Recognition** – object recognition, motion tracking, stereomapping, and character recognition.
3. **Medical Image Analysis** – medical diagnosis and biomedical research.

In general, image registration contains three essential steps: (1) control points selection, (2) control points pairing, (3) mapping function estimation. Usually, control points pairing is the most difficult step. Thus, how to accomplish control points pairing (or point pattern matching) is discussed more often in the literature. A correlation-based method is not capable of matching rotated and scaled images except that the rotation- and scaling-invariant features can be extracted before correlation, or that the observed image can be approximately

* Corresponding author. E-mail: ycchen@ee.nthu.edu.tw.

[1] Electronic Annexes available. See http://www.elsevier.nl/locate/patrec.

PII S0167-8655(97)00010-X

rotated to match the orientation of the reference image before template matching. However, rotation- and scaling-invariant feature extraction is much involved and initial rotation estimation is not easy to achieve without any control points pairing procedure.

Ranade and Rosenfeld (1980) proposed the relaxation method for point pattern matching, which is merely capable of solving the translation problem. Ogawa (1984) proposed the fuzzy relaxation method, by which labeled point sets with translation, rotation and scaling can be registered. Flusser and Suk (1994) proposed a control points pairing approach based on affine moment invariants (AMI). It is known that moment computing is time-consuming and susceptible to noise degradation. Goshtasby et al. (1986) employed a clustering technique to determine the correspondence between two sets of control points. Flusser (1995) utilized the shape matrix as the feature of a segmented region to evaluate the "matching likelihood coefficient" for the achievement of pairing. Skea et al. (1993) proposed a control points matching algorithm which employs the invariant properties of sphericity and centroid translation. However, the matching algorithm can only be used for those images with translation. The problem of point pattern matching originates from two-dimensional photometry, and from matching star lists in the area of astronomy. Murtagh (1992) proposed an algorithm for matching star lists based on the proximity of feature vectors associated with the coordinate couples in lists. The method is robust when magnitudes of stars are utilized.

The control points pairing method of this paper is based on line segments incorporating any two control points, which is applicable to the registration of images with variant rotation, scaling and translation. By using two invariant properties, a 2-D histogram is established and the most possible pair of segments will be found. Thus, the pairing of control points can be easily achieved. The proposed image registration system is introduced in Section 2. The most important part of registration, i.e., control points pairing, is discussed in Section 3. Section 4 demonstrates the experimental results using synthetic control points and authentic images, respectively. Finally, conclusions are drawn in Section 5.

2. Hierarchical image registration system

Image registration by a hierarchical method has been proposed in (Zheng and Chellappa, 1993). The system is able to reduce the registration complexity and obtain an accurate estimate of transformation parameters. The architecture of our proposed hierarchical system is illustrated in Fig. 1. The registration procedure involves several steps.

Step 1. Construct the image database I_1^i and I_2^i, where I_1 is the reference image, I_2 is the observed image and the superscript i is the image resolution index with $i = 1, \dots, Q$. Q represents the total number of resolution steps in the database. I^1 has the lowest resolution and I^Q has the original resolution. I_1 and I_2 are related by rotation, scaling and translation (i.e. similarity transform) which can be represented in the form of Eq. (A.4).

Step 2. Extract the control point sets P_1^1 and P_2^1 as the centroids of closed-boundary regions in I_1^1 and I_2^1, respectively. Note that P_j^i contains the control points which are mapped onto the domain of resolution i, i.e., the control point (x, y) of P_j^i is equivalent to $(2x, 2y)$ of P_j^{i+1} (if the downsampling factor is 2).

Step 3. Proceed control points pairing by AL (angle difference and line-length ratio) histogram. This step is under our principal discussion in Section 3.

Step 4. Estimate the transformation parameters $\omega(i)$ and $\Omega(i+1)$, $\omega(i)=(s(i), \theta(i), x(i), y(i))$, $\Omega(j)=(\hat{s}(j), \hat{\theta}(j), \hat{x}(j), \hat{y}(j))$. s and $\hat{s}$ denote the scales between two images. θ and $\hat{\theta}$ depict the rotation angles. (x, y) and $(\hat{x}, \hat{y})$ represent the translations. $\omega(i)$ is estimated by control point sets P_1^i and P_2^i. $\Omega(j)$ is successively evaluated by accumulating $\omega(i)$, $0 < i < j$. The parameters of $\Omega(i+1)$ are evaluated by the following equations which are clarified in Appendix A.

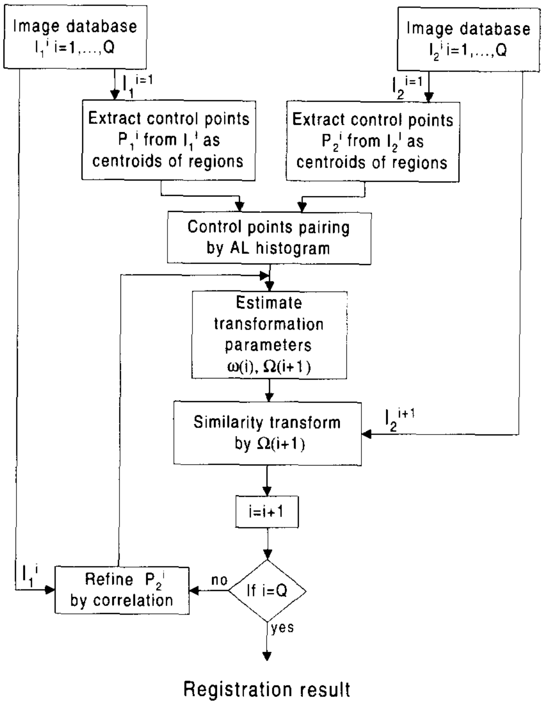

Fig. 1. The hierarchical satellite image registration system diagram.

$$\hat{s}(i+1) = \prod_{j=1}^{i} s(j), \quad i > 0, \tag{1}$$

$$\hat{\theta}(i+1) = \sum_{j=1}^{i} \theta(j), \quad i > 0, \tag{2}$$

$$\hat{T}(i+1) = \begin{cases} \gamma T(i), & i = 1, \\ \sum_{j=1}^{i-1} \left\{ \left[\prod_{k=j+1}^{i} s(k) \right] \bar{\theta}(j+1, i) \gamma^{i+1-j} T(j) \right\} + \gamma T(i), & i > 1, \end{cases} \tag{3}$$

$$T(i) = \begin{bmatrix} x(i) \\ y(i) \end{bmatrix}, \qquad \hat{T}(i) = \begin{bmatrix} \hat{x}(i) \\ \hat{y}(i) \end{bmatrix}, \tag{4}$$

$$\bar{\theta}(m,n) = \begin{bmatrix} \cos\phi(m,n) & \sin\phi(m,n) \\ -\sin\phi(m,n) & \cos\phi(m,n) \end{bmatrix}, \qquad \phi(m,n) = \sum_{k=m}^{n} \theta(k), \tag{5}$$

where γ denotes the downsampling factor between I^{i+1} and I^i.
Step 5. Apply similarity transform to I_2^{i+1} and P_2^{i+1} with $\Omega(i+1)$.
Step 6. Increase image resolution: $i = i + 1$.
Step 7. Exit the system if $i = Q$, otherwise refine P_2^i by correlation coefficient and go back to Step 4.

In the database, there are three resolutions of images, i.e., $Q = 3$. The dimension of I^3 is 1024×1024. By using the downsampling factor $\gamma = 2$, the dimension of I^1 is 256×256. With this smaller image, the time consumption of the control points extraction and the registration complexity can be much reduced.

The control points selection can be accomplished manually or automatically. In automatic methods (Goshtasby, 1988), control points are usually selected as the centers of window having locally maximum variances, line intersections, or points of locally maximum curvature on contours. In recent years, many authors have employed the centroids of closed-boundary regions (Goshtasby et al., 1986) as control points because they are fairly stable under random noise degradation or gray-level variations (Flusser and Suk, 1994). In Step 2, the control point sets P_1^1 and P_2^1 are evaluated as the centroids of regions in I_1^1 and I_2^1, respectively. The regions of interest might be segmented regions or areas with high contrast (Flusser and Suk, 1994).

3. Control points pairing algorithm

In this section, the control points pairing algorithm is proposed for image registration. First, two invariant properties are defined in Section 3.1, by which every true pair of line segments (one line segment from the reference image, and the other from the observed image) will accumulate one vote on the cell of a 2-D AL histogram (discussed in Section 3.2). The cell will report the most possible angle and scale between the reference and the observed images. By using a simple pairing procedure (introduced in Section 3.3), the control points pairing can be achieved.

3.1. The invariant properties

For correct and rapid pairing, it is necessary to exploit or identify the invariant properties which are easy to be defined, to be employed, and to characterize the mapping between two sets of control points. Without the invariant properties, the pairing cannot be accomplished by the control points alone. Before giving the definition of the invariant properties, the control point sets and the line segment sets are introduced first. By such line segments, two invariant properties can be identified.

The point sets of the reference image I_1^1 and the observed image I_2^1 are given in Eqs. (6) and (7). Each point (P_{1i} or P_{2i}) is the centroid of a closed-boundary region. Note that the control points extraction is merely performed (in Step 2 of the proposed registration system) once in the lowest resolution images, i.e., I_1^1 and I_2^1.

$$P_1^1 = \{P_{1i} = (x_{1i}, y_{1i}) \mid i = 1, \ldots, N_1\}, \tag{6}$$

$$P_2^1 = \{P_{2i} = (x_{2i}, y_{2i}) \mid i = 1, \ldots, N_2\}. \tag{7}$$

From point sets P_1^1 and P_2^1, we have the sets of line segments (L_{1i} and L_{2i}) of image 1 and image 2, respectively.

$$\xi_1 = \{L_{1i} = (P_{1j}, P_{1k}) \mid j, k = 1, \ldots, N_1,\ j \neq k,\ i = 1, \ldots, C_2^{N_1}\}, \tag{8}$$

$$\xi_2 = \{L_{2i} = (P_{2j}, P_{2k}) \mid j, k = 1, \ldots, N_2,\ j \neq k,\ i = 1, \ldots, C_2^{N_2}\}, \tag{9}$$

where N_i is the number of control points in image I_i^1.

By using any possible pair of line segments from two images, two invariant properties are defined. The first invariant property of line segments is defined as the line-length ratio of any two line segments in image 1 and image 2, respectively. Let R_{jk} be the line-length ratio of line segment L_{1j} (from image 1) and L_{2k} (from image 2),

$$R_{jk} = \rho_1 \log(d(L_{1j})/d(L_{2k})), \quad j = 1, \ldots, C_2^{N_1}, \quad k = 1, \ldots, C_2^{N_2}, \tag{10}$$

where $d(L)$ denotes the length of line segment L and ρ_1 is a given constant. If the abscissa value of the peak of the line-length ratio histogram equals x, all the $R_{mn} = x$ have the most pairing possibility that line segments L_{1m} and L_{2n} be a pair.

The second invariant property is defined as the angle difference. The angle difference of line segments of image 1 and image 2 is defined as

$$A_{jk} = \rho_2[\theta(L_{1j}) - \theta(L_{2k})], \quad j = 1, \ldots, C_2^{N_1}, \quad k = 1, \ldots, C_2^{N_2}, \tag{11}$$

where $\theta(L)$ is the orientation of the line segment L and ρ_2 is a given constant. Based on the same principle as the first invariant property, all the pairs (L_{1m}, L_{2n}), whose angle differences A_{mn} equal the abscissa value of the peak of the angle histogram, are likely to be correct pairs.

3.2. The line-related 2-D AL histogram and matching

Having defined two invariant properties: the line-length ratio and the angle difference, we establish the 2-D AL histogram from these two invariant properties in this subsection. From the 2-D histogram, all possible pairs of line segments can be found. The 2-D histogram is established by the following steps.

Step 1. Compute all the line-length ratios R_{mn} and the angle differences A_{mn}, $m = 1, \ldots, C_2^{N_1}$, $n = 1, \ldots, C_2^{N_2}$.
Step 2. Construct table $T_s(m,n)$; $m = 1, \ldots, C_2^{N_1}$, $n = 1, \ldots, C_2^{N_2}$. $T_s(m,n) = (R_{mn}, A_{mn})$ is evaluated from line segment L_{1m} and L_{2n} by Eqs. (10) and (11).
Step 3. Establish the 2-D AL histogram from table T_s.

Now that the 2-D AL histogram is constructed, the matching table of control points is formed by the following two steps.

Step 1. From the 2-D histogram, find out the maximum value, and its corresponding line-length ratio $R_{mn} = \bar{R}$, angle difference $A_{mn} = \bar{A}$. Any $T_s(m,n) = (\bar{R}, \bar{A})$, the line segment pair (L_{1m}, L_{2n}) is selected as a candidate of a possible correct pair.
Step 2. Suppose $L_{1m} = (P_{1j_1}, P_{1k_1})$, $L_{2m} = (P_{2j_2}, P_{2k_2})$, and $T_c(j,k)$ is a matching table for control points, $j = 1, \ldots, N_1$, $k = 1, \ldots, N_2$. The four cells (corresponding to these four control points) of T_c accumulate one vote, i.e., $T_c(j,k) = T_c(j,k) + 1$, $j = j_1, j_2$, $k = k_1, k_2$. The value in cell (j,k) denotes the possibility that the (j)th control point P_{1j} of image 1 and the (k)th control point P_{2k} of image 2 could be a pair.

Now we have the matching table T_c (dimension $= N_1 \times N_2$), from which the reasonable pairing can be determined by a simple "scanning algorithm".

3.3. The pairing procedure

This subsection discusses how to decide the reasonable pairing from table T_c. The pairing procedure is described below.

Step 1. Each row is scanned for finding the maximum value and set others to zero.
Step 2. Each column is scanned for finding the maximum value and set others to zero.
Step 3. Control points P_{1j} and P_{2k} can be considered to form a correct pair if the following criteria are satisfied.

1. $T_c(j,k) \neq 0$.
2. $T_c(j,k) > t_1$ and $T_c(j,k) > t_2$. $t_i = c(M_i/N_i)$, $i = 1,2$. M_i is the number of line segments of set i which can be selected as the candidates, i.e., the values (R_{mn}, A_{mn}) of those line segments equal $(\bar{R}, \bar{A})$. N_i is the number of control points of image i. c is a constant for adjustment. $c = 0.5$ is chosen in our system.

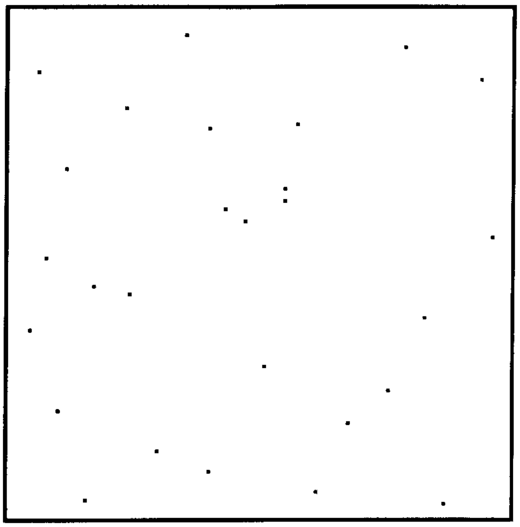

Fig. 2. The reference control point pattern of the first set, scale = 1.0, angle = 0.0°.

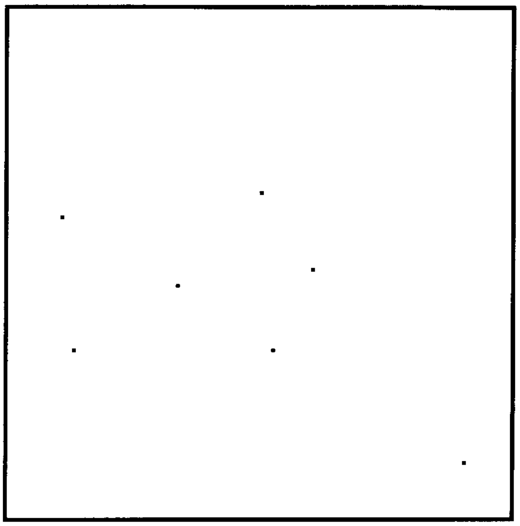

Fig. 3. The control point pattern of the first set, scale = 1.4, angle = 45.0°.

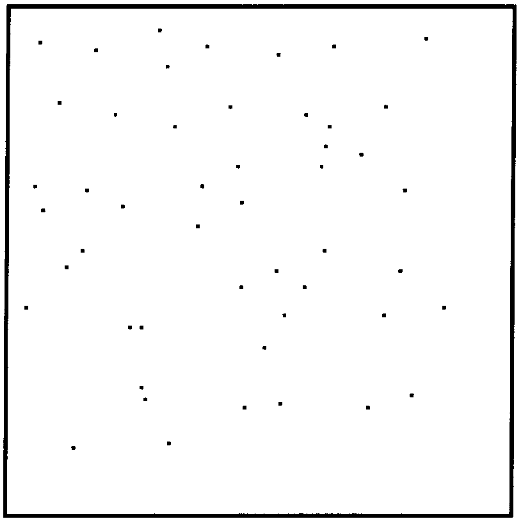

Fig. 4. The reference control point pattern of the second set, scale = 1.0, angle = 0.0°.

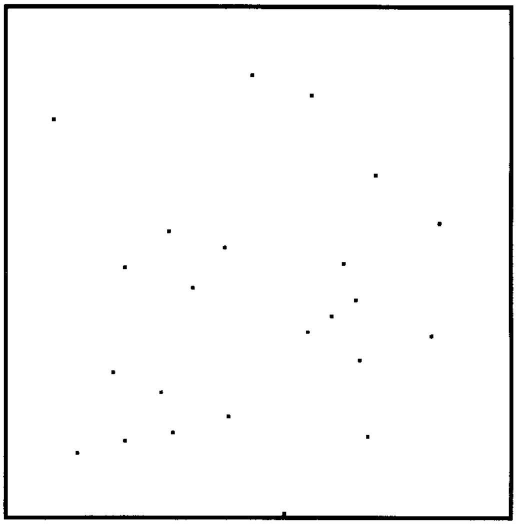

Fig. 5. The control point pattern of the second set, scale = 1.4, angle = 45.0°.

It is noted that $C_2^{N_i}$ may be huge if N_i is large. In order to limit the number of line segments and acquire a reasonable computation load, the number of control points must be constrained. In general, N_i may range from 3 to 30. Evidently, large N_i is expected to bring about considerable amount of line segments and increase the possibility of false pairing and the computation load of pairing. Nevertheless, tiny N_i may result in poor estimation of transformation parameters due to (1) the poor model-fitting by the least square, and (2) the gross error of some control points. In addition, the reduction of control points in an image is also effected by scaling and rotation of the image. The detail discussion of the number of control points and the computation load of the proposed method is presented in Section 4.3. As a result, 10 to 15 tends to be a proper number of control points for the proposed pairing method.

Table 1
The pairing results of the first set of control points

Scale	Angle difference	Line-length ratio	AL
0.4	(6,6,0.333)	(15,15,0.833)	(15,15,0.833)
0.6	(7,7,0.389)	(12,11,0.556)	(15,15,0.833)
0.8	(12,12,0.667)	(14,14,0.778)	(17,17,0.944)
1.0	(16,16,0.941)	(15,14,0.768)	(16,16,0.941)
1.2	(1,0,−0.083)	(7,0,−0.583)	(10,10,0.833)
1.4	(5,0,−0.714)	(5,1,−0.429)	(5,5,0.714)
1.6	(3,0,−0.500)	(4,0,−0.667)	(5,5,0.833)
av. MI	0.148	0.179	0.847

Table 2
The pairing results of the second set of control points

Scale	Angle difference	Line-length ratio	AL
0.4	(0,0,0.000)	(28,27,0.703)	(27,27,0.730)
0.6	(18,18,0.500)	(24,23,0.611)	(28,28,0.778)
0.8	(30,30,0.833)	(30,29,0.778)	(34,34,0.944)
1.0	(31,31,0.886)	(27,27,0.711)	(33,33,0.943)
1.2	(27,27,0.871)	(19,18,0.548)	(30,30,0.968)
1.4	(18,18,0.720)	(10,0,−0.400)	(14,14,0.560)
1.6	(10,10,0.454)	(11,0,−0.500)	(21,21,0.955)
av. MI	0.609	0.350	0.840

4. Experiments and discussions

First, two sets of computer-generated control points are tested. One of them contains 27 points and the other is composed of 49 points. It is shown that the proposed pairing method can successfully achieve pairing and acquire high reliability. The second experiment demonstrates the results of the hierarchical registration system (Fig. 1) which incorporates the proposed control points pairing algorithm. Finally, discussion is presented for the appropriate number of control points and comparison with AMI method.

4.1. Pairing results of synthetic control points

The first set of computer-generated control points contains 8 point patterns including the reference one which is made up of 27 points and is given in Fig. 2 with scale = 1.0, angle = 0°. All other synthetic point patterns of the first set are generated from Fig. 2. Fig. 3 (scale = 1.4, angle = 45° corresponding to Fig. 2) is one example of the first set. It is produced by (1) randomly deleting 8 points from Fig. 2, (2) magnifying a factor of 1.4, and (3) rotating 45° counterclockwise. The pairing results for the first set of point patterns are given in Table 1.

The second set of the synthetic point patterns also consists of 8 point patterns. The reference point pattern is composed of 49 points and is given in Fig. 4 with scale = 1.0, angle = 0°. Fig. 5 (scale = 1.4, angle = 45° corresponding to Fig. 4) is an example of the second set. It is generated from Fig. 4 by the same way of the first set. The pairing results for the second set of point patterns are given in Table 2.

The second column of each table shows the pairing results only by the angle difference. The third column shows the pairing results only by the line-length ratio. The last column gives the pairing results by the proposed method. The values (x,y,z) shown in the tables are explained as follows.

1. x is the paired number by the used method.
2. y is the number of correct pairings, $(x-y)$ is the number of false pairings.
3. z is the matching index (MI) to evaluate the pairing accuracy of the employed method. $z=(y-(x-y))/N$, $z \in (-1,1)$. N is the number of common points (the maximum number of possible pairings). $z=1$ denotes the best performance. $z=-1$ depicts that the method is subject to the worst pairing.

The average values of MI of the proposed method are 0.847 and 0.840 for the first and the second set, respectively. These are much higher than those only by means of the angle difference or the line-length ratio. In addition, the MI of point patterns of various scales does not vary too much. This shows the reliability of our method. Hence, it is obvious that a single invariant property may result in rather poor pairing for some point patterns. With two invariant properties, it seems to have fairly good capability for correct point matching.

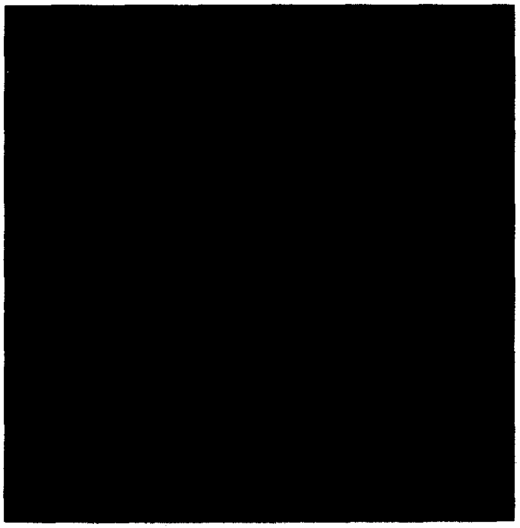

Fig. 6. The reference image with control points (indicated by "+" mark).

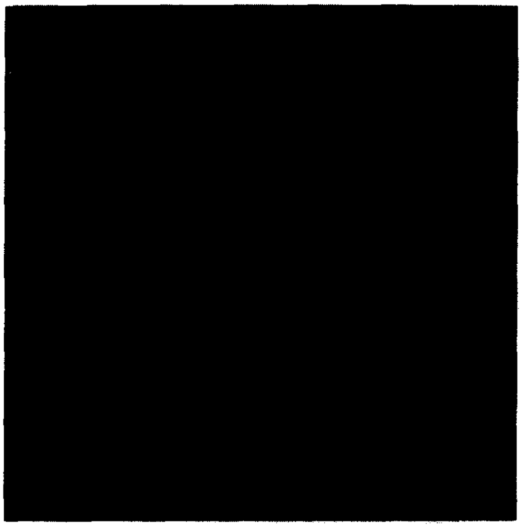

Fig. 7. The extracted regions of the reference image.

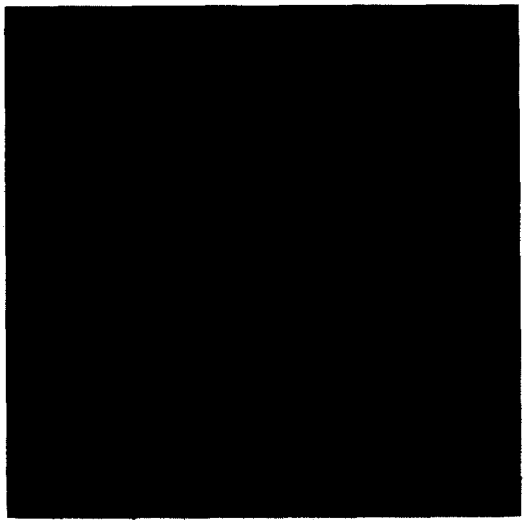

Fig. 8. The observed image with control points (indicated by "+" mark). The image has scale = 0.8 and rotation angle = 30° corresponding to the reference image.

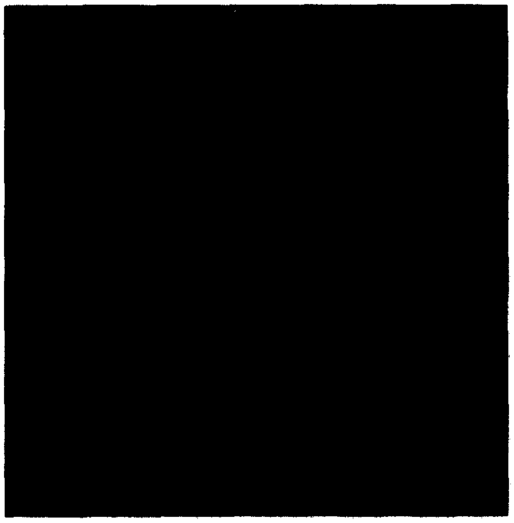

Fig. 9. The extracted regions of the observed image.

Table 3
The coordinates of the control points

For the reference image					For the observed image		
a1 = (236,13)	a2 = (6,33)	a3 = (115,59)	a4 = (110,67)	a5 = (146,67)	b1 = (188,19)	b2 = (163,27)	b3 = (164,35)
a6 = (99,82)	a7 = (225,114)	a8 = (121,119)	a9 = (200,136)	a10 = (126,144)	b4 = (161,49)	b5 = (205,82)	b6 = (121,214)

4.2. Registration results of satellite images

In this experiment, real satellite images are utilized. The database of Fig. 1 involves three resolutions of images. They are I_1^1, I_1^2 and I_1^3 for the reference image, I_2^1, I_2^2 and I_2^3 for the observed image. I_1^3 and I_2^3, whose dimensions are 1024×1024, are the subscenes of SPOT satellite image where I_2^3 is to be registered with I_1^3. We choose the downsampling factor $\gamma = 2$ so that the dimensions of I_1^2 and I_2^2 are 512×512 and the dimensions of I_1^1 and I_2^1 are 256×256. It is noted that the selection of the downsampling factor γ may affect the computation load and the registration accuracy. The larger the γ is, the larger the registration error will be.

Fig. 6 shows the subsampled version I_1^1 of the reference satellite image I_1^3. Convolved with Sobel operators, the high contrast areas of I_1^1 are extracted with binarization by threshold 120. These areas are shown in Fig. 7. By using a contour-tracing algorithm, ten centroids of the closed-boundary regions, whose perimeters are between 10 and 100 pixels (Flusser and Suk, 1994), are selected as the control points in Fig. 6. Fig. 8 shows the subsampled version I_2^1 of the observed satellite image I_2^3. The high contrast areas of I_2^1 are shown in Fig. 9. The number of control points in Fig. 8 is 6. The coordinates of these control points are listed in Table 3. Consequently, there are 4 pairs of control points in total by virtue of the proposed pairing algorithm, i.e., Step 3 of our registration procedure. The 4 pairs are (a3, b2), (a4, b3), (a6, b4), and (a10, b5).

For the analysis of correctness of the pairing, the only way is to compare two sets of transformation parameters. One set is estimated by these four pairs of control points. The other set is estimated by manually selected and paired control points. On the other hand, the registration accuracy of the hierarchical registration system is also analyzed. In Step 4 of the registration procedure (discussed in Section 2), the transformation parameter $\omega(1)$ is estimated from control point sets P_1^1 and P_2^1 containing these 4 pairs of control points. The transformation parameters are evaluated as

$$\omega(1) = (0.81, 29.88, 161.44, 44.97). \tag{12}$$

Note that the true parameters are (scale = 0.80, angle = 30.00, $x = 161.72$, $y = 46.08$) which are estimated by manually selected and paired control points. The similarity transform is then applied to I_2^2 with $\Omega(2)$. $\Omega(2)$ is evaluated as

$$\hat{s}(2) = s(1), \quad \hat{\theta}(2) = \theta(2), \quad \hat{x}(2) = \gamma x(1), \quad \hat{y}(2) = \gamma y(1), \tag{13}$$

$$\Omega(2) = (0.81, 29.88, 322.88, 89.95), \tag{14}$$

by substituting $i = 1$ into the equations in Step 4 of the registration procedure.

After transforming and refining each control point's position of P_2^2 (Step 7 of the registration in Section 2) by a correlation coefficient (Zheng and Chellappa, 1993), $\omega(2)$ is estimated from P_1^2 (which have been adjusted for resolution 2 from resolution 1) and the new P_2^2 as

$$\omega(2) = (1.00, 0.13, 1.85, 0.76). \tag{15}$$

From the values of $\omega(2)$, it is clear that the residual geometric distortion between I_1^2 and I_2^2 is small (note that the I_2^2 has been transformed with $\Omega(2)$ as listed in Eq. (14)). Eventually, the similarity transform is applied to I_2^3 with $\Omega(3)$. $\Omega(3)$ is evaluated by $\omega(1)$ and $\omega(2)$ from Eqs. (1), (2) and (3). The transformation parameters for resolution 3 are calculated as

$$\hat{s}(3) = s(1)s(2), \tag{16}$$

$$\hat{\theta}(3) = \theta(1) + \theta(2), \tag{17}$$

$$\begin{bmatrix} \hat{x}(3) \\ \hat{y}(3) \end{bmatrix} = s(2) \begin{bmatrix} \cos\theta(2) & -\sin\theta(2) \\ \sin\theta(2) & \cos\theta(2) \end{bmatrix} \gamma^2 \begin{bmatrix} x(1) \\ y(1) \end{bmatrix} + \gamma \begin{bmatrix} x(2) \\ y(2) \end{bmatrix}, \tag{18}$$

$$\Omega(3) = (0.80, 30.00, 647.71, 182.51). \tag{19}$$

Note that the true transformation parameters between I_1^3 and I_2^3 are (0.80, 30.00, 647.88, 184.32).

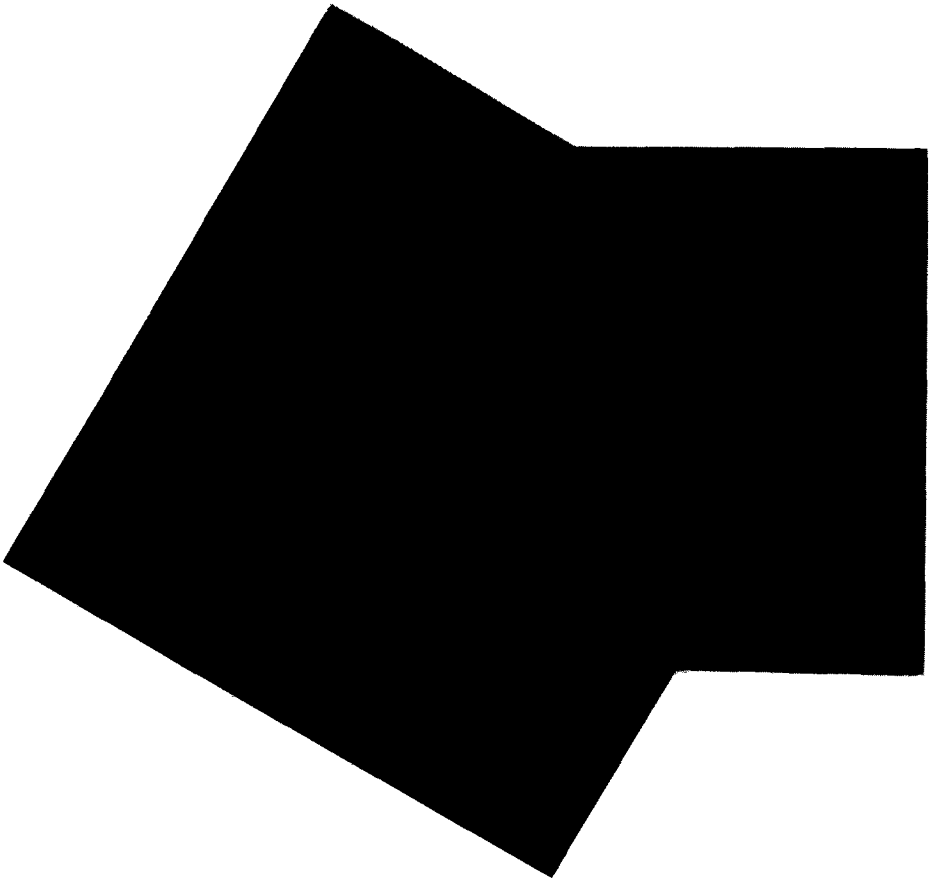

Fig. 10. The registration result.

By the above step-by-step evaluations of the hierarchical registration system (as shown in Fig. 1), the overall registration result (the overlap of I_1^3 and similarity transform of I_2^3 with $\Omega(3)$) is acquired and demonstrated in Fig. 10. For the analysis of registration accuracy, the average registration error ε is given as

$$\varepsilon = \frac{1}{N^2} \sum_{j=1}^{N} \sum_{i=1}^{N} \left[(x(i,j) - x'(i,j))^2 + (y(i,j) - y'(i,j))^2 \right]^{1/2}, \tag{20}$$

where N is the dimension of an image, (i,j) is the original coordinate of the observed image, $(x(i,j), y(i,j))$ is the coordinate of the observed image after transformation with the correct transformation parameters, and $(x'(i,j), y'(i,j))$ denotes the coordinate of the observed image after transformation with the estimated transformation parameters. $\varepsilon = 0.65$ pixels in the case the similarity transform is applied to I_2^1 with $\omega(1)$, which is equivalent to 2.60 pixels in 1024×1024 image domain. In Fig. 10, $\varepsilon = 1.42$ pixels. It is obvious that the hierarchical registration result is correct and accurate.

4.3. The comparison with the AMI method

Now we discuss the computation load of the proposed control points pairing method. Table 4 lists the computation load for the AMI method (Flusser and Suk, 1994) (including the computation of centroids) of all regions of interest. Assume that an extracted region is a square, then its dimension is $N \times N$. N_1 and N_2

Table 4
The amount of computation load of AMI and centroids. The first value ($n1$) in the parenthesis is for "add" or "subtract". The second value ($n2$) in the parenthesis is for "multiply", "divide" or "power"

	$N_1 = N_2 = 10$	$N_1 = N_2 = 15$	$N_1 = N_2 = 20$
$N = 5$	(10240,6460)	(15360,9690)	(20480,12920)
$N = 10$	(40240,19960)	(60360,29940)	(80480,39920)
$N = 15$	(90240,42460)	(135360,63690)	(180480,84920)

Table 5
The amount of computation of centroids and two invariant properties. The first value (n1) in the parenthesis is for "add" or "subtract". The second value (n2) in the parenthesis is for "multiply" or "divide"

	$N_1 = N_2 = 10$	$N_1 = N_2 = 15$	$N_1 = N_2 = 20$
$N = 5$	(3435,220)	(13515,480)	(39920,840)
$N = 10$	(6435,220)	(18015,480)	(45920,840)
$N = 15$	(11435,220)	(25515,480)	(55920,840)

denote the number of control points of the reference and the observed images, respectively. Let us denote the total amount of "add" or "subtract" computation by $n1$,

$$n1 = (N_1 + N_2)(20N^2 + 12); \tag{21}$$

and the total amount of "multiply", "divide", or "power" computation by $n2$,

$$n2 = (N_1 + N_2)(9N^2 + 98). \tag{22}$$

Table 5 lists the computation load for the proposed method including the evaluations of centroids, angle differences, and line-length ratios. It is assumed that the computations of "$\tan^{-1}$" and "log" can be accomplished by tables. The total amount of "add" or "subtract" computation is

$$n1 = (N_1 + N_2)(2N^2 - 2) + 5(C_2^{N_1} + C_2^{N_2}) + C_2^{N_1}C_2^{N_2}. \tag{23}$$

The total amount of "multiply" or "divide" computation is

$$n2 = 2(N_1 + N_2) + 2(C_2^{N_1} + C_2^{N_2}). \tag{24}$$

From Tables 4 and 5, it is evident that most of the computation loads of AMI are much larger than those of the proposed method. Because a high-order central moment is susceptible to noise degradation, the elements of AMI are of low orders. Nevertheless, they have poor capability to distinguish between the details of shapes. In addition, if N is small, it is difficult to distinguish between similar shapes, which will result in poor shape matching. Hence, N should not be too small, e.g. $N > 5$. However, if N is large, the computation load of AMI will be very enormous. Therefore, from the inspection of the row of the tables that $N = 10$ and the consideration of the computation load of the proposed method, the appropriate number of control points is between 10 to 15.

5. Conclusions

A control points pairing algorithm has been proposed in this paper. This method is based on two invariant properties between two sets of line segments which are comprised of the control points of the reference and the observed images, respectively. By means of the invariant properties, the scale and the rotation between two images can be easily found from a 2-D histogram and the pairing can be achieved in the sequel without complicated computation. The method is simple and more efficient than AMI method. Although AMI method can deal with the problem of rotation and scaling, it is more time-consuming than the proposed method according to the analysis of computation load. In addition, AMI method cannot distinguish between similar shapes, which may result in wrong pairing. The performance of the proposed method has been demonstrated by experiments on the synthetic point sets. It has shown that a correct pairing and high matching index is attainable even if some control points are missing in one point pattern. Moreover, the pairing algorithm is also tested for the remotely sensed satellite images in a hierarchical registration system. The pairing result is correct and leads to an accurate transformation parameters estimation. From the experiments and the above discussions, it is clear that the method is suitable for practical implementation.

Appendix A

$\omega(i)$ is defined as the transformation parameter estimated by control point sets P_1^i and P_2^i. $\Omega(j)$ is the eventual transformation parameter used for transformation of I_2^j. Thus, $\Omega(j)$ is the combination of $\omega(i)$, $i < j$. It is assumed that I_2^4 is to be registered with I_1^4. Hence, it is required to evaluate $\Omega(4)$.

First, $\omega(1)$ is estimated by P_1^1 and P_2^1. Thus, the first transformation for I_2^4 is

$$[s(1), \theta(1), \gamma^3 x(1), \gamma^3 y(1)]. \tag{A.1}$$

After transforming I_2^2 by $\Omega(2)$ and refining P_2^2, $\omega(2)$ is estimated, by which the second transformation for I_2^4 is

$$[s(2), \theta(2), \gamma^2 x(2), \gamma^2 y(2)]. \tag{A.2}$$

After transforming I_3^2 by $\Omega(3)$ and refining P_3^2, $\omega(3)$ is estimated, by which the third transformation for I_2^4 is

$$[s(3), \theta(3), \gamma x(3), \gamma y(3)]. \tag{A.3}$$

The first transformation for I_2^4 is

$$\begin{bmatrix} x' \\ y' \end{bmatrix} = s(1) \begin{bmatrix} \cos\theta(1) & -\sin\theta(1) \\ \sin\theta(1) & \cos\theta(1) \end{bmatrix} \begin{bmatrix} x \\ y \end{bmatrix} + \begin{bmatrix} \gamma^3 x(1) \\ \gamma^3 y(1) \end{bmatrix}. \tag{A.4}$$

The second transformation is

$$\begin{aligned} \begin{bmatrix} x'' \\ y'' \end{bmatrix} &= s(2) \begin{bmatrix} \cos\theta(2) & -\sin\theta(2) \\ \sin\theta(2) & \cos\theta(2) \end{bmatrix} \begin{bmatrix} x' \\ y' \end{bmatrix} + \begin{bmatrix} \gamma^2 x(2) \\ \gamma^2 y(2) \end{bmatrix} \\ &= s(1)s(2) \begin{bmatrix} \cos(\theta(1)+\theta(2)) & -\sin(\theta(1)+\theta(2)) \\ \sin(\theta(1)+\theta(2)) & \cos(\theta(1)+\theta(2)) \end{bmatrix} \begin{bmatrix} x \\ y \end{bmatrix} \\ &\quad + s(2) \begin{bmatrix} \cos\theta(2) & -\sin\theta(2) \\ \sin\theta(2) & \cos\theta(2) \end{bmatrix} \begin{bmatrix} \gamma^3 x(1) \\ \gamma^3 y(1) \end{bmatrix} + \begin{bmatrix} \gamma^2 x(2) \\ \gamma^2 y(2) \end{bmatrix}. \end{aligned} \tag{A.5}$$

The third transformation is

$$\begin{aligned} \begin{bmatrix} x''' \\ y''' \end{bmatrix} &= s(3) \begin{bmatrix} \cos\theta(3) & -\sin\theta(3) \\ \sin\theta(3) & \cos\theta(3) \end{bmatrix} \begin{bmatrix} x'' \\ y'' \end{bmatrix} + \begin{bmatrix} \gamma x(3) \\ \gamma y(3) \end{bmatrix} \\ &= s(1)s(2)s(3) \begin{bmatrix} \cos(\theta(1)+\theta(2)+\theta(3)) & -\sin(\theta(1)+\theta(2)+\theta(3)) \\ \sin(\theta(1)+\theta(2)+\theta(3)) & \cos(\theta(1)+\theta(2)+\theta(3)) \end{bmatrix} \begin{bmatrix} x \\ y \end{bmatrix} \\ &\quad + s(2)s(3) \begin{bmatrix} \cos(\theta(2)+\theta(3)) & -\sin(\theta(2)+\theta(3)) \\ \sin(\theta(2)+\theta(3)) & \cos(\theta(2)+\theta(3)) \end{bmatrix} \begin{bmatrix} \gamma^3 x(1) \\ \gamma^3 y(1) \end{bmatrix} \\ &\quad + s(3) \begin{bmatrix} \cos(\theta(3)) & -\sin(\theta(3)) \\ \sin(\theta(3)) & \cos(\theta(3)) \end{bmatrix} \begin{bmatrix} \gamma^2 x(2) \\ \gamma^2 y(2) \end{bmatrix} + \begin{bmatrix} \gamma x(3) \\ \gamma y(3) \end{bmatrix} \\ &= \left[\prod_{k=1}^{3} s(k)\right] \bar{\theta}(1,3) \begin{bmatrix} x \\ y \end{bmatrix} + \left[\prod_{k=2}^{3} s(k)\right] \bar{\theta}(2,3)\gamma^3 T(1) + \left[\prod_{k=3}^{3} s(k)\right] \bar{\theta}(3,3)\gamma^2 T(2) + \gamma T(3). \end{aligned} \tag{A.6}$$

Let $i = 3$. Then we have $\Omega(4) = (\hat{s}(4), \hat{\theta}(4), \hat{x}(4), \hat{y}(4))$,

$$\hat{s}(4) = \prod_{j=1}^{3} s(j), \tag{A.7}$$

$$\hat{\theta}(4) = \sum_{j=1}^{3} \theta(j), \tag{A.8}$$

$$\begin{aligned} \hat{T}(4) &= \left[\prod_{k=2}^{3} s(k)\right] \bar{\theta}(2,3)\gamma^3 T(1) + \left[\prod_{k=3}^{3} s(k)\right] \bar{\theta}(3,3)\gamma^2 T(2) + \gamma T(3) \\ &= \sum_{j=1}^{i-1} \left\{ \left[\prod_{k=j+1}^{i} s(k) \right] \bar{\theta}(j+1, i)\gamma^{i+1-j} T(j) \right\} + \gamma T(i). \end{aligned} \tag{A.9}$$

References

Brown, L.G. (1992). A survey of image registration techniques. *ACM Computing Surveys* 24 (4), 325–376.

Flusser, J. (1995). Object matching by means of matching likelihood coefficients. *Pattern Recognition Letters* 16 (9), 893–900.

Flusser, J. and T. Suk (1994). A moment-based approach to registration of images with affine geometric distortion. *IEEE Trans. Geoscience and Remote Sensing* 32 (2), 382–387.

Goshtasby, A. (1988). Image registration by local approximation methods. *Image and Vision Computing* 6 (4), 255–261.

Goshtasby, A., G.C. Stockman and C.V. Page (1986). A region-based approach to digital image registration with subpixel accuracy. *IEEE Trans. Geoscience and Remote Sensing* 24 (3), 390–399.

Murtagh, F. (1992). A new approach to point-pattern matching. *Publications of the Astronomical Society of the Pacific* 104, 301–307.

Ogawa, H. (1984). Labeled point pattern matching by fuzzy relaxation. *Pattern Recognition* 17 (5), 569–573.

Ranade, S. and A. Rosenfeld (1980). Point pattern matching by relaxation. *Pattern Recognition* 12, 269–275.

Skea, D., I. Barrodale, R. Kuwahara and R. Poecker (1993). A control point matching algorithm. *Pattern Recognition* 26 (2), 269–276.

Zheng, Q. and R. Chellappa (1993). A computational vision approach to image registration. *IEEE Trans. Image Processing* 2 (3), 311–325.